The influences of environmental conditions on source localisation using a single vertical array and their exploitation through ground effect inversion

Roland Kruse, Shahram Taherzadeh
The Open University, Department of Design, Development, Environment and Materials, MK7 6AA Milton Keynes, UK

Abstract

The performance of microphone arrays outdoors is influenced by the environmental conditions. Numerical simulations indicate that, while horizontal arrays are hardly affected, direction-of-arrival (DOA) estimation with vertical arrays becomes biased in presence of ground reflections and sound speed gradients. Turbulence leads to a huge variability in the estimates by reducing the ground effect. Ground effect can be exploited by combining classical source localization with an appropriate propagation model (ground effect inversion). Not only does this allow the source elevation and range to be determined with a single vertical array but also it allows separation of sources which can no longer be distinguished by far field localization methods. Furthermore, simulations provide detail of the achievable spatial resolution depending on frequency range, array size and localization algorithm and show a clear advantage of broadband processing. Outdoor measurements with one or two sources confirm the results of the numerical simulations.

Keywords: Source localization, Ground effect inversion, Outdoor sound propagation

Introduction

Microphone arrays are a tool for localization and separation of sound sources and suppression of background noise. Commercially important applications include hearing aids, handsfree sets in vehicles and conference rooms as well as localization of noise sources, traffic monitoring and security applications outdoors.
Typically, outdoor source localization is characterized by a source-array distance which is much larger than the array size. Thus, and because of its computational efficiency, localization methods are generally based on a free field, far field assumption, and a single array can only estimate the direction of arrival (DOA) of the incident sound. Source distance is obtained by triangulation using DOAs from two or more spatially separated arrays [1] or, preferably, by combining the data from these arrays directly [2]. In individual cases, it is possible to get distance estimates even with a single array by exploiting range dependent changes in the waveform, e.g. in case of supersonic sources generating shock waves, an example being shooter detection. In the same situation, the delay between shock wave and muzzle blast may be exploited for range estimation [3].
Source height estimation, on the other hand, would require vertically separated arrays in a free field, far field scenario, something that is at least inconvenient if not impossible in many situations. A free field is a greatly simplified description of the sound propagation in the atmosphere, several factors effect it.
In fig.1, an overview is given of these phenomena. The direct wave is overlaid with the one reflected by the ground. Sound speed gradients caused by thermal layering of the atmosphere as

well as wind shear change the inclination of the wave fronts. Turbulence leads to random fluctuations of sound pressure and phase. As a result, the wave front arriving at the array is distorted, phase (and pressure) relations between the microphone positions, which are the basis for any source localization technique, have changed in a deterministic (ground reflection, sound speed gradients) and random (turbulence) way. Additionally, absolute sound levels will increase or decrease depending on frequency.
As atmospheric sound propagation is historically well understood, a large number of models exist taking into account several or all of the above mentioned factors as well as others not considered here like irregular terrain or obstacles. For the purpose of this study it is sufficient to notice that for any situation there will be a (physical) model which predicts the complex propagation loss between source and receiver with arbitrary accuracy, and that these models will differ significantly in their computational efficiency.
In connection with source localization it is important to remember that these techniques rely on the phase difference (and, less often, on the level difference) between closely spaced microphones. The absolute sound level, which is the subject of numerous studies on the effect of environmental conditions on noise propagation, has only a secondary effect on the array's performance by changing the signal to noise ratio (SNR) and consequently the uncertainty of the DOA estimation. Unfortunately, there's a distinctive lack of investigations of both numerical and experimental nature on the specific influence of the environmental conditions on the performance of microphone arrays outdoors or, in other words, on their performance under under non-ideal conditions. Furthermore, there is a focus on the effect of turbulence, although “Other physical phenomena, such as ground reflections and refraction by atmospheric wind and temperature gradients, are not considered in this analysis and may have a considerable impact on the ability to estimate the elevation.“ [4]. Even scarcer than theoretical and numerical results are measurements under realistic environmental conditions. Atmospheric refraction and turbulence lead to serious drop in spatial coherence [5] so that the use of large aperture arrays is no longer advisable even though these would offer an excellent performance under ideal conditions. Further measurements under moderately complex propagation conditions [6] support these results and show that, for low frequencies, small arrays have not the necessary spatial sensitivity, on the other hand very large arrays are affected by turbulence and do also not provide an optimal performance.
To gain a better understanding of which factors influence the performance of microphone arrays when used for source localization and to develop an improved method for outdoor source localization, especially source height determination, we will in a first step check which factors have the widest influence on DOA estimation accuracy. This will be done by combining sound propagation models of increasing complexity with classical source localization methods to calculate the DOA misestimation for a number of geometries, frequencies and environmental conditions, both for horizontal and vertical linear arrays.
In a second step, the effect of one of the (major) factors in outdoor sound propagation, the ground reflection, will be exploited to improve the localization methods and enable them to detect both the source elevation and range with a single vertical array of microphones even if the source is in the far field. This method – ground effect inversion - will consequently be an example of matched field processing popular in underwater acoustics. In a limited fashion this strategy has been used by [7] for solving the problem addressed here, source height estimation. However, the authors assumed the source distance to be known and used solely the difference in levels between the microphones instead of exploiting the phase differences as classical DOA estimation does.
This study comprises both numerical simulations and outdoor measurements for their verification.

Experimental procedure

A multi-step approach, involving numerical simulations and outdoor measurements, has been used in this investigation. An overview the entire approach will be given first followed by details of the experimental procedure.
In the first step, the influence of three main factors in outdoor sound propagation, ground reflection, vertical sound speed gradients and turbulence, on DOA estimation with horizontal and vertical arrays has been analysed by numerical simulation. For that purpose, the complex propagation loss from the source to the array microphones has been calculated for a wide range of frequencies, source positions, microphone spacings and ground impedances as listed in table 1. An array of

eight equally- spaced microphones was assumed. Then, these propagation losses were applied to single frequency test signals and spatially white noise has been added to achieve an SNR of 20 dB. DOAs have been estimated from these sets of signals by use of two different source localization algorithms which by itself assumed a free field, far field situation. Estimated DOAs were subsequently compared with actual DOAs to determine what factors have the highest effect on the accuracy of source localization.
In the second step, the source localization methods have been modified to include the effect of ground reflection. While it is popular to assume far field propagation without ground reflection, because this leads to computationally efficient localization algorithms – in some situations to search free algorithms – even the conventional techniques used in this investigation can be combined with more sophisticated propagation models. This will, in theory, not only eliminate any possible bias the ground reflection causes in DOA estimation but it will also allow the source position (range and elevation) to be identified with a single vertical array. The adequacy of the refined localization procedure was again tested by numerical simulation for one or two sound sources for both single frequency and broadband signals. Attention was paid to the attainable spatial resolution, the choice of the frequency range and uniqueness of the solution. In addition, the influence of the SNR on the variability of the range and elevation estimates has been examined, and it was checked how sensitive the ground effect inversion is to inaccurate ground impedance estimates.
In a third step, the predictions were verified by outdoor measurements with a single vertical array of eight equally-spaced microphones. Different source positions as well as source signals were considered, and measurements were done with one or two sources. From the data, the source elevation was estimated using conventional (far field) localization procedures as well as the suggested improved procedure including the effect of ground reflection, which in addition provided estimates of the source range.
An exp(+iωt) time dependence is understood. Vectors are column vectors, ^{H} denotes complex transpose. All calculations and the data acquisition were done using Matlab R2009b.

Propagation models

Predicting sound propagation outdoors requires the use of propagations models. The choice and complexity of a model depends on which factors it should include and which assumptions are made. In this study, two different models were used, and axial symmetry was assumed to allow for an efficient calculation. Consequently, the model will predict the sound pressure (equal to the propagation loss for a source of unity strength) on a vertical plane just as the sketch in fig.2 indicates. In addition, a flat, locally reacting ground with range independent impedance is presumed.
In case of a homogeneous atmosphere (speed of sound is position independent), the sound field of a point source above an impedance plane can be found analytically using eq.1 [8, eq.30].

$$L(f,G,Z)=\frac{e^{-ikr_1}}{r_1}+Q(f,G,Z(f))\frac{e^{-ikr_2}}{r_2} \tag{1}$$

with propagation loss L, frequency f, geometry G (source height h_s, range R, receiver height h_r), ground impedance Z, length of direct path r_1, length of reflected path r_2, wave number k and spherical wave reflection coefficient Q.

A two-parameter model (eq.2) [9] described the frequency dependent impedance of the ground for three different ground types: soft ground (pine forest floor), hard ground (compacted silt) [10] and medium impedance ground (compacted lawn) [11].

$$Z_c=\frac{1}{\sqrt{\pi\gamma\rho_0}}\sqrt{\frac{\sigma_e}{f}}(1-i)-i\left(\frac{c_0\alpha_e}{8\pi\gamma f}\right) \tag{2}$$

with characteristic impedance Z_c, adiabatic index of air γ, air density ρ_0, effective flow resistivity σ_e, effective change of porosity with depth α_e and speed of sound c_0

Equation 1 was used to calculate the propagation loss between source and array microphones in absence of vertical sound speed gradients and turbulence. In addition, the free field case (Q = 0) was considered. It is important to note that, in the time domain, the received signal is the sum of the direct signal and the delayed (and attenuated) ground reflection, with the ground reflection getting weaker with increasing frequency due to the decreasing impedance of the ground.
If the speed of sound varies locally, the sound field generally has to be predicted using a numerical model, and a wide angle, Crank-Nicholson parabolic equation (CNPE) scheme as described in [12] was used. The grid spacing was $\lambda/10$, being, if necessary, reduced to make sure that source and receivers were on grid points. The number of vertical layers corresponded to a maximum height of (h_s + R /5), with a minimum number of layers of 500, plus 500 absorbing layers at the top. The starting field was of second order. Validity of the CNPE implementation was checked by comparing it with the analytical model and by comparison with benchmark cases [13].
CNPE was used to model two different situations. One the one hand, vertical sound speed gradients were introduced by changing the speed of sound with height according to eq. 3.

$$c(z) = c_0 + b \ln\left(1 + \frac{z}{z_0}\right) \tag{3}$$

with speed of sound at height z above the ground c, b = +1 (downward refraction) resp. -1 (upward refraction) and z_0 = 0.1 m.

On the other hand, turbulence was modelled by multiplying the speed of sound field with a Gaussian random field with a variance (mean squared index of refraction) of 10^{-5} and a correlation length of 1 m indicating medium strong turbulence [14]. To take into account that turbulence is not only a spatial but also a temporal phenomena, the sound field was calculated for 25 realizations of the random field.
The (complex) propagation losses for the eight microphone positions were calculated for all parameter combinations from table 1, for the free field situation, the homogeneous atmosphere (only ground reflection), downward and upward refracting atmosphere and downward refraction plus turbulence. The results were stored together with the parameters for subsequent use.

Source localization

Source localization with arrays can be achieved with a great number of different schemes. Two classical methods, representing two different classes of localization algorithms, have been selected as they can be used for arbitrary array geometries and can be straightforwardly extended to broadband processing. All processing has been done in the frequency domain.
The first method is steered response power (SRP) with the delay-and-sum beamformer. The output variance of this beamformer is given by eqs.4 and 5 [15].

$$R(f) = X(f)\,X(f)^H \tag{4}$$

$$\Phi(\theta) = \sum_f a(f,\theta)^H R(f)\, a(f,\theta) \tag{5}$$

with array response function a, steering direction θ, covariance matrix R, observed amplitude matrix for each microphone and timeframe X and beamform power Φ (variance of the signal).

Once the steering direction is equal to the direction-of-arrival, the phase differences between the microphone signals will be compensated by a_H and Φ will become maximal. The method is search based, and the maximum of Φ was found by calculating Φ on a $1/4^{th}$ deg. grid.
The array response vector a is the (phase) response of the array to a signal from a specific direction (or, more generally, source location). In the far field case, a is given by eq.6, representing the phase differences caused by the (geometric) path length differences.

$$a(f,\theta) = e^{i k d \cdot \sin\theta} \tag{6}$$

with the vector of distances of the microphones from the reference microphone (microphone 1) d.

SRP with delay-and-sum beamformer is robust, but has limited and frequency dependant spatial resolution depending directly on the width of the main lobe of the beamformer.
Therefore, MUSIC (Multi- Signal Classification) as a high resolution subspace method has also been used (eq.8) [16]. It is based on the eigendecomposition of the signal covariance matrix (eq.7). The matrix of eigenvectors is then partitioned into the matrix of eigenvectors corresponding to the n (number of sources) largest eigenvalues (the signal subspace) and the (m-n), m being the number of microphones, lowest eigenvalues (the noise subspace). The noise subspace is orthogonal to a_H (and the signal subspace), so that the DOA is found by searching for the direction which makes
a_H U minimal. To allow for a better comparison with SRP, we will maximize the inverse of this product and call it pseudo beamform power Φ_{MUSIC}. Note that, unlike Φ, it has no physical meaning. MUSIC can provide a very high spatial resolution, but only at high SNR. MUSIC will not work correctly when used on single time frames (snapshots) [17].

$$R(f) = U S U^H \tag{7}$$

$$\Phi_{MUSIC}(\theta) = \sum_f \frac{1}{a(f,\theta)^H (\bar{U}(f)\bar{U}(f)^H) a(f,\theta)} \tag{8}$$

with matrix of eigenvectors *U*, diagonal matrix of eigenvalues *S*, submatrix of *U* corresponding to (m-n) lowest eigenvalues $\bar{U}$ (noise subspace), pseudo beamform power Φ_{MUSIC}.

Time difference of arrival (TDOA) based position estimation

In case the source is in the near field of the array, the time difference of arrival between the microphones depends on the source position and not only on the DOA as in a far field scenario. The TDOA can be determined from cross correlation of the (filtered) microphone signals. As long as the ground reflection is weaker than the direct signal and holds a minimum delay relative to it one can expect that the cross correlation will provide the delay between the direct signals only. Source position is obtained by comparing the observed time differences with the ones predicted by a free field model (eq.1 with Q = 0) where the delays arise solely from path length differences. An (inverse) least squares estimator [18] (eq.9) has been used to allow comparison with the methods already presented.

$$\Phi_{TDOA}(G) = 1/\sum_{i=2}^{m} (\tau_{1,i} - \bar{\tau}_{1,i})^2 \tag{9}$$

with pseudo beamform power Φ_{TDOA}, number of microphones *m*, observed delays rel. to microphone 1 $\tau_{1,i}$, predicted delays $\bar{\tau}_{1,i}$.

TDOA based position estimation is very fast, but will become unreliable once the source is in the far field and the additional delays cause by the finite source- array distance become smaller than one sample.

Ground effect inversion

The two localization algorithms presented can be extended to arbitrary propagation models by replacing the far field array response vector (eq.6) with one corresponding to the respective model as specified in eq.10. The response vector is the ratio of the propagation loss to it's magnitude, or, in other word, the array's phase response vector. In this study, the analytical solution for a homogeneous atmosphere (eq.1) was used as it's still computationally efficient.

$$a(f,G,Z) = \frac{L(f,G,Z)}{|L(f,G,Z)|} \tag{10}$$

Unlike the far field case, where the array response depends on only one unknown parameter – the

DOA – it is now a function of source height , range and ground impedance. In case of the numerical simulation, the exact ground impedance has been used. For the outdoor measurements, the ground impedance was estimated to conform to a 2PA model with σ_e = 100 krayl/m and α_e = 40 m^{-1} typical of (slightly compacted) lawn.

Source position was determined with a grid search over beamform power Φ on a grid with a $1/4_{th}$ deg spacing for the elevation and 60 grid points on an exponential scale between minimum and maximum source- array distance, which in this investigation was 5 - 50 m. In case of multiple sources, this procedure will only find the strongest one. Therefore, it was in addition checked if there was a value of the beamform power ϕ which would separate the spatial patterns of the sources and correctly border the actual locations of the sources.
The same grid has been used for TDOA based position estimation to allow for a direct comparison of the methods.

Influence of SNR

The influence of SNR on the variability of the source range and elevation estimates has been investigated for the geometries, microphone spacings and ground impedances in tab.1. The corresponding transmission losses (eq.1) have been applied to bandpass filtered pink noise of one second length and the signals were mixed with (spatially) white noise to obtain an SNR (in the given frequency range) between -20 and 20 dB. The signals have been preprocessed as described in the next chapter and the source positions have been estimated by ground effect inversion. To allow for a more efficient computation, this has been done on a 33 * 33 grid spanning ± 2 deg resp. ± 50% of the source distance. From the estimates, the relative errors (in %) in source range and the errors in elevation (in deg.) have been calculated. The percentage of combinations from tab.1 with an error in the range of less than 10% or an error in elevation of less than 0.5 deg has been used as an indicator of the variability of the position estimates due to the noise.
This simulation was done for height of the lowest microphone of 1 meter. In addition, it was done for microphone heights of 2 and 5 meters keeping the source height (not the DOA) the same as in the 1 meter case.

Influence of the ground impedance

The ground impedance is an input parameter in the propagation model and therefore needed for ground effect inversion. The impedance (or the parameters of an impedance model) are normally unknown, though estimates for different grounds can be found in the literature, e.g. [19]. To investigate the influence of the chosen impedance on the accuracy of the position estimation a similar procedure as for influence of the SNR has been used. Now, the sound field at the array has been calculated with the “correct” impedance, but the position estimation has been done with the flow resistivity changed by (-50, -20, 0, +50, +100) %. SNR was 40 dB, so that estimation errors are a result of the wrong impedance (systematic errors) and not of the noise (random errors).
The same description of the resulting error, the percentage of combinations of geometry, frequency range, ground impedance and flow resistivity error for which the error in range is less than 10% and the error in elevation less than 0.5 deg. has been used.

Outdoor measurements

To verify the results of the numerical simulation and the performance of the ground effect inversion, measurement on a cricket field have been done on two different days. On the first day, measurements with a single source and three ranges and two heights were done. A vertical array consisting of eight 1/2” type 1 microphones with windscreens, spaced 20 cm apart, was used, with the lowest microphone one meter above the ground. Microphones were connected to a preamplifer with a tenfold amplification, ICP power supply, 50 Hz high pass and 4 kHz low pass filter. The amplified signals were fed into a PC using an USB data acquisition card with a sampling frequency of 50 kHz and 16 bit resolution. The source signals consisted of a series of single tones at 100, 250, 500 and 1000 Hz and pink noise, each segment five seconds long. At each position, two measurements were done, the second one with the source level reduced by about 6 dB. In

addition, the background noise – mostly from the ventilation system of nearby buildings and cars / lorries passing at low speed - was sampled before each measurement to get an estimate of the SNR.
On the second day, two identical sources were used. A test sequence consisted of only source 1, only source 2 or both sources emitting pink noise with the same power. Furthermore, the level of the second source was reduced or increased by 6 dB leading to five segments of five seconds length plus five seconds of background noise. For this experiment, the microphone spacing has been increased to 50 cm.
While wind speeds were low (< 2 m/s at 2 m height) during both days, they were slightly higher during the second one. In addition, there was a higher difference between night time and day time temperature during this day so that one may expect higher (but still low) turbulence during the second day.
Time data was stored for later processing. For the source position estimation, four seconds of the recordings, starting one seconds after the begin of playback, were divided into $1/10_{th}$ second frames. Then, the spectra for each microphone and frame were calculated, restricted to the source frequency (single tones) or the frequency range later given (pink noise) and subsequently the frequency dependent covariance matrices were obtained. These covariance matrices were then fed into the localization algorithms.
For TDOA estimation, the delays relative to microphone 1 were found from the maximum of the cross correlation of the unsegmented, bandpass filtered (+/- 5 Hz for the narrowband signals, 500 - 4000 Hz for the pink noise) time signals.

Results

The results of the numerical simulations as well as the experimental data will be presented in the same order as in the previous section. First, the influence of outdoor conditions on (narrowband) DOA estimation will be analysed. Then, examples of source position estimation by ground effect inversion are presented for one or two sources. Finally, the results of the outdoor measurements are shown.

Influence of environmental conditions on DOA estimation

All results presented in this section are from SRP with the delay-and-sum beamformer. The MUSIC results were identical within the chosen angular resolution of ¼ deg.

Ground reflections

The influence of the ground reflection on the DOA estimation with horizontal arrays is shown in fig.2. It shows the distribution of the differences between actual and estimated direction-of-arrival for all parameter combinations except the ones with a microphone spacing larger than λ/2 which may exhibit spacial aliasing. For approx. . of all parameter combinations, the error is not larger than 1 deg, with a maximum error of approx. 7 deg. In the same situation without ground reflections, similarly sized errors were observed with the highest errors for the largest array and the smallest source- array distance (“near field effect”). The maximum additional error cause by the ground reflection was 3.25 deg.
The situation is completely different for vertical arrays as shown in fig.3. The errors cover a much larger range of up to almost 80 deg. Errors of more than 10 deg are common. In fig.4, another example of this “ground effect” is given for one specific geometry and ground impedance. The figure shows the beamform power (SRP and MUSIC) versus frequency (in 1/3 octave bands) along with the DOA estimates. One can see that the DOA estimates are highly frequency dependent, esp. below 500 Hz. Below 150 Hz, the spatial resolution of the delay-and-sum beamformer is very low, MUSIC provides a significant better resolution. Additional simulations show, however, that MUSIC will not lead to an improvement for a SNR (in the frequency band) of less than 3 dB.

Sound speed gradients

The effect of a vertical, logarithmic sound speed gradient is pictured in fig.5. It shows the difference

between the downward refracting and upward refracting situation as a kind of worst case scenario. While there is a noticeably effect, it is much smaller than the ground effect (fig.3) with errors larger than 10 deg only occurring in less than 10% of all cases.

Turbulence

Turbulence causes fluctuations in the DOA estimates as presented in fig.6. The variability

increases remarkably with increasing ground impedance and, for each impedance group, with source- array distance (which rises stepwise from 15 to 100 m from left to right). The standard deviation can become as large as 90 deg. Not shown but noteworthy is the fact that the mean error in the presence of turbulence is often not much different from the error in the same situation without turbulence.

Source position determination by ground effect inversion

Selected results from the simulation of the source position estimation by ground effect inversion will now be presented. The chosen geometries agree with later measurements. Unless noted otherwise, simulations are for a vertical array of eight microphones, spaced 20 cm, with the lowest microphone one meter above the ground.

Single source

Simulation results for a single source at a range of 15 m and a height of 3.68 m are given in figs.7-9 showing maps of (pseudo) beamform power Φ versus range and elevation. For a single tone at 250 Hz in white noise and a SNR of 10 dB (fig.7) the spatial resolution is very poor, and though MUSIC improves the resolution it's still low. Using a larger array with a 50 cm spacing, on the other hand, led to a significant improvement. The source position is detected correctly in all cases.
In fig.8, the same situation for a 2 kHz tone is illustrated. Resolution is much better, but an unwanted, extended local maximum around 40 m range occurs. While even in this case the source position is detected correctly, the maximum at 40 m is almost as high as the one at 15 m, and especially if the noise level was increased an incorrect source position of 40 m and 9 deg was occasionally found. This was also true for MUSIC in the same situation.
In fig.9, beamform power is shown for pink noise. If a frequency range of 50 – 4000 Hz is used, spatial resolution is low, and using only the 500 – 4000 Hz range results in a significant improvement. Spectral MUSIC will further increase resolution considerably and, unlike in the 2 kHz situation, the broadband signal produces a well defined maximum without undesirable secondary maxima.
In all examined situations, the spatial resolution for the elevation is much better than the one for the range.

Two sources

In figs.10 and 11, examples for the localization of two broadband sources of equal strength are given. In the first case, pink noise sources at the same distance of 15 m, but heights of 2 and 3.7 m, were to be detected. As fig. 10 demonstrates, the two sources are well separated even for delay-and-sum SRP ($\phi = 0.8$). The grid search found the strongest source at a distance of 16.2 m and a height of 2.1 m, but would also randomly select the second source.
If the sources are at the same height (1.5 m) but at a different distance (15 or 24 m), the situation is more complicated as indicated in fig. 11. The search found a source at 15.5 m and 1.5 m height. The sources were still separable with delay-and-sum SRP with a threshold of $\phi = 0.9$. In this situation, MUSIC did only locate the closest source correctly.
It should furthermore be noted that for these two geometries the “normal” far field MUSIC DOA was able to separate the sources (the DOA versus frequency diagram would “fork”) at different heights for frequencies above 1.6 kHz, whereas it was not able to distinguish the sources having the same height within the given frequency range of up to 4 kHz, even with the large array.

Influence of SNR

The influence of the SNR on the variability of the source position estimates is presented in tab.2. It gives the percentage of combinations of the parameters in tab.1 which showed an error in the range of less than 10% or an error in elevation of less than 0.5 deg, respectively. Only arrays with a minimum microphone spacing of λ/10 (for the center frequency) were included in the calculation. Results are for MUSIC based position estimation. The percentage of combinations increases clearly with increasing SNR and with increasing frequency range. The percentage of combinations for an elevation error of less than 0.5 deg is only in 5 out of 28 combinations of SNR and frequency range lower than the percentage for a range error of less than 10%. In case of the low SNR of -20 dB, the percentage are below 50% for all frequency ranges. For an SNR of at least 5 dB, these percentages are, with one exception, above 80% and often even above 90%.
A closer inspection of the data reveals that the two percentages will furthermore increase with increasing microphone spacing. The percentage of range errors of less than 10% decreases with increasing range. There's no clear influence of the elevation except from a drop in the percentage of elevation errors of less than 0.5 deg for 0 deg. incidence. No influence of the ground impedance is noticeable.
If delay-and-sum SRP is used instead of MUSIC, the results show the same trend. MUSIC had an advantage over SRP for range estimation of, on average, 9 percent points, with low SNR / low frequency combinations benefiting most. On the other hand, SRP estimates the elevation angle more reliably leading to an average increase in the percentage of combinations with an estimation error of less than 0.5 deg of 2 percent points. In this case there's no clear relationship between improvement and SNR / frequency range combination.
Results for a height of the lowest microphone of 2 or 5 meters not presented here show the same trends. Variability for the array at 2 meters height was clearly lower compared to the array at 1 meter height, for both the range and the elevation estimation. Increasing the array height to 5 meters led to a further improvement in the range estimation but to an increase in the variability of the DOA estimation to values less good than in the 1 m case.

Influence of the ground impedance

The influence of a difference in the actual flow resistivity of the ground and the one used for the ground effect inversion in shown in tab.3. As in the previous chapter, shows the percentage of combinations of the parameters in tab.1 which showed an error in the range of less than 10% or an error in elevation of less than 0.5 deg, respectively. All results are for delay-and-sum SRP. The last column (All) shows the percentages if one combined all levels of the error in the flow resistivity (including the error free case) and is therefore a measure of these percentages if the flow resistivity error was in the range of -50 to +100 %.
The percentages increase clearly with increasing frequency, and (not shown) with increasing microphone spacing, increasing ground impedance, decreasing source-array distance and, for the elevation estimates, increasing elevation angle.
An error of -50% has roughly the same effect as an error of +100%. Percentages for the elevation estimates within ± 0.5 deg. are higher than for range estimates within ± 10%. Combined percentages range from 75% (range estimates, 50 – 250 Hz) to 99% (elevation, 2 – 4 kHz) for an array at 1 meter height.
If the array height is increased to 2 meters, the combined percentage range changes to 84 – 99%, for an array at 5 meters to 96 – 100%.

Outdoor measurements

Results of the verification measurements done on a lawn will now be presented for one or two sources and for the small (20 cm spacing) and large array (50 cm spacing).

Background noise and SNR

Background noise was broadband with low frequencies dominating. On the first day, at the lowest microphone, it started with 32 db (Pa/√Hz), decreasing to 11 dB at 500 Hz, a slight increase to 19

dB at 1 kHz followed by a steep decline to -14 dB at 4 kHz. Noise was similar on the second day with slightly more low frequency components and less high frequency ones.
SNR for the narrowband signals ranged from 0 – 20 dB at 100 Hz increasing to 30 – 52 dB at 2 kHz. For the pink noise on day 1, it ranged from 3 to 18 dB, on the second day from 8 to 19 dB.

Single source

An overview of the direction-of-arrival estimates for the small array obtained with the far field assumption is given in table 4. The mean estimation error for all measurements is 4 deg for the 100 Hz signal and 2.2 – 2.6 deg for all other signals, including the broadband one. There's no clear relationship between source position and size of error.
In table 5, the results of the source position estimation including ground effect are given. For the sake of comparison, estimates using free field TDOA (eq.9) are provided in the same table, but only for the broadband signal as delay estimation between periodic signals suffers from non uniqueness. Because of the low spatial resolution below 500 Hz, estimates for these frequencies are not shown. The mean error in source elevation is highest for 500 Hz (2.8 deg) and lowest for 1 kHz (0.4 deg) and pink noise (0.3 deg). TDOA based source localization led to an average error of 0.8 deg. In comparison with conventional far field source localization, the errors in estimated elevation are drastically lower.
The error in source range varies from 9 m (500 Hz and TDOA) to 3.2 m (1 kHz and pink noise). The error tends to increase with increasing range, especially for TDOA based localization.
Table 6 shows the estimated source positions for the large array and a single source. The error is higher than the one for the first measurement with the smaller array, with an average error of 0.6 deg and 5.7 m. TDOA based position estimation led to a higher average error in the estimated elevation (1.2 deg) but a lower error in the source- receiver distance (3.4 m). Far field, free field direction-of-arrival estimation showed a very high average error of 12.2 deg, with the lowest error for the highest elevation angle of 10.1 deg; had one reasonably limited the search to positive elevation angles the estimated elevation would be 0 deg for all geometries except the one with the source at a height 3.7 m, the average error would then be 2 deg.
For both arrays, the ground effect inversion tended to underestimate source distances.
An example of a beamform power “map” is presented in fig.12 for pink noise between 500 – 4000 Hz , a source at a distance of 15 m and an elevation of 10.1 deg and the small array. The source position can clearly be identified, indicating a range of 12.3 m and an elevation of 10.3 deg. MUSIC provided basically the same result but severely reduced the source's “footprint”.
The same measurement, done with the large array, has the same result but the larger aperture reduced the source's footprint significant.

Two sources

In fig.13, the beamform power map for two broadband sources is shown, the first source at a distance of 15 m and an elevation of 10.1 deg, the second source at 15 m, 3.8 deg. Note that a beamform power range of 30 – 100 % of the maximum has been used, whereas a range of 70 – 100 % has been used before. The sources generate a similar maximum beamform power and can easily be distinguished even with delay-and-sum SRP.
Fig.15 shows a more complicated situation. While the source at a distance of 15 m can easily be detected, the second one at 24 m generates a much lower maximum ϕ. Still, with a threshold of ϕ =
0.4, the areas belonging to the two sources can be separated. With MUSIC, discrimination of the sources is possible for even lower thresholds.
Fig.14 shows the most complicated situation encountered during the measurements. The sources are at the same height of 1.5 m at distances of 15 resp. 24 m. The level of the second sources is reduced by 6 dB. In this case with almost the same DOA, separation is no longer possible with delay-and-sum SRP. MUSIC is able to correctly detect the sources with a threshold of $\phi = 0.6$.
For all 24 combinations of geometry and source power ratios, at least MUSIC position estimation was able to separated the sources and located them close to their actual positions. TDOA based position estimation detected in 19 cases one source correctly, in the other 5 cases it indicated a position not agreeing with any of the two sources. These were cases were the level of the two sources (at the array) was similar.

Discussion

The numerical simulations reveal, first of all, that there's a remarkable difference in the influence of typical outdoor environmental conditions on the performance of vertical and horizontal arrays. Horizontal arrays for DOA finding are hardly affected by ground reflections, using the far field assumption when indeed the source is in the near field has a higher effect. Vertical arrays, on the other hand, are severely affected and failure to include the ground effect in the DOA estimation - or use methods insensitive to it - will often lead to unusable elevation estimates.

Sound speed gradients can have a moderate effect on DOA estimation within the investigated source range of not more than 100 m as they lead to tilting of the wave fronts. With the 2D propagation model used, it was not possible to determine the effect of horizontal sound speed gradients, however, these gradients tend to be considerably smaller than vertical ones [12] and consequently vertical arrays would again be influenced most.

Turbulence, even of moderate magnitude, causes distinct fluctuations of the DOA estimates which increase with range and ground impedance, with additional simulations not presented here showing that the variability practically vanishes in absence of a ground reflection. The strong dependence on the impedance or, in other words, the reflection coefficient of the ground, suggests this is an indirect effect: turbulence changes the correlation between direct and reflected wave. Thus, the sound pressure and phase as a result of the interference between these two components will vary [20], the ground effect will change. As the ground effect has a strong influence on vertical arrays, turbulence will inevitably cause a huge variability in DOA estimates. As horizontal arrays are barely affected by the ground reflection, this will also mean that there are barely affected by turbulence. In this context it's important to remember that source localization as presented in this paper relies on the phase relation between the microphones and not on the absolute level or phase. Turbulence will, even in a free field, change the absolute phase between source and receiver, but it will not change the phase relation between two locations if their separation is significantly smaller than the scale of the turbulence. Very large arrays not considered in this investigation may however be influenced especially if the source- array distance is large.

Inclusion of the ground effect in DOA estimation, then becoming position estimation, leads to a substantial increase in source localization accuracy. The simulations for a single source indicate that a reasonable spatial resolution with an eight element array and 20 cm spacing can be achieved for frequencies of more than 500 Hz, whereas a larger array is recommended for lower frequencies. Resolution of the elevation is better than resolution of the range. Resolution increases with increasing frequency, but one has to expect unwanted additional maxima of the beamform power in case of narrowband processing. As a consequence, broadband processing is advantageously as it leads to a well defined maximum at the source position. This is especially important if more sophisticated search methods (not an inefficient search on a fixed grid) are used because they may get trapped in local maxima.

Simulations for two (uncorrelated) sources show that sources of similar power and distance, but different height can be distinguished easily. While this is also possible by “normal” far field DOA estimation, ground effect inversion allows, in addition, sources with similar DOA but at different distances to be separated.

Use of super-resolution methods like MUSIC can increase the spatial resolution quiet severely and allow for separating of more closely spaced sources. They're, especially for broadband processing, only marginally less computational efficient: the eigendecomposition has to be done only once. Even for low SNRs of -10 dB or less they lead to a lower variability in the position estimates compared to delay-and-sum SRP, though variability can still high. However, for such low SNRs they offer almost no improvement in the spatial resolution.

Performance of the position estimation by ground effect inversion depends on the frequency range chosen. Given a constant array size, increasing the frequency increases the change of beamform power with changing source position. Consequently, the method becomes more robust to unwanted influences like noise. At the same time, the method becomes more robust to an inaccurately chosen ground impedance / flow resistivity. Another reason for this effect is the fact that the impedance (and hence the reflection coefficient) of natural grounds varies more in the low frequency range than for higher frequencies. Increase of sensitivity to changes in the source position (or DOA) with increasing frequency occurs also in a free field situation, but in the presence of ground there's an additional influence of the height of the array above the ground, and

increasing the height to 2 meters reduces both the variability of the position estimates and the sensitivity to an incorrect ground impedance. A further increase in height to 5 meters has, on the other hand, a negative influence on the elevation angle estimation.
The results of the numerical simulations are backed by the measurement data. For the small array and a single source, the simulated source map (fig.9) agrees well with the measured one (fig.12). In this case, DOA estimation with far field assumption gave an average accuracy of not less than 1.5 deg (for pink noise), whereas an accuracy of 0.3 deg has been observed for broadband processing with ground effect. Accuracy of range estimation is less good but still within a few meters, with a tendency for underestimation. TDOA based source localization, in comparison, exhibited a worse performance than ground effect inversion except for the 500 Hz narrowband signal. With the source range becoming much larger than the array size, TDOA range estimates, esp. for sources close to the ground, became inaccurate for higher distances as shall be expected because this method relies on the additional delays cause by the source being in the near field. With the large array, the far field DOA estimation now suffers from both near field and ground effect leading to poor accuracy (2.3 deg). Indeed, it did often indicate negative DOAs which were, for the sake of comparison with the other methods, and knowing that the source height was never below 1 m, set to 0. TDOA based position estimation, on the other hand, did benefit from the increased array size which was almost $1/10_{th}$ of the maximum array- source distance and showed a quiet decent performance (1.3 deg resp. 3.6 m). Still, ground effect inversion gave the best elevation estimates (0.6 deg), even though the error was higher than for the small array. This does surprise as an array with higher aperture should not only offer better spatial resolution – which it did – but also lower variability of DOA estimates assuming all other factors like SNR are similar. One can only suspect that the higher susceptibility of the large array to turbulence together with a higher atmospheric turbulence itself (higher wind speeds) led to a decreased performance.
Measurements with two sources demonstrate one of the main advantages of the proposed method: it is able to separate sources which have a similar DOA, but different array- source distances, and can consequently not be distinguished by standard DOA estimation. This is most easy if the sources are of comparable level (at the array) so that they have comparable maximum beamform powers. In this case, the threshold for Φ can be chosen as close to 1 and the footprints of the sources become very small so that even closely spaced sources can be discriminated. One the other hand, if one source is substantially weaker than the other and the distance between them is low, separation may no longer be possible even with MUSIC. The example shown in fig.14 seems to be close to the maximum performance one may anticipate. However, one can still expect the ground effect inversion to correctly localize the strongest source. In contrast, TDOA based localization has problems with multiple sources of similar level, as in this case the estimated delays between the pairs of microphones may not necessarily belong to the same source and, as a result, the indicated source position may not agree with any of the sources.
As long as the SNR of the weaker source is still sufficiently high to allow its detection in absence of the stronger source, one may use a CLEAN [21] like strategy to localize it: removal of the strongest source from the covariance matrix. This can be achieved by using its eigendecomposition (eq.8) and deleting the largest eigenvalues and the associated eigenvector. Alternatively, after obtaining the location *G* of the strongest source, one can estimate its power spectrum *s(f)* by use of eq.11, calculate the covariance matrix R_S of this source and subtract it from the total covariance matrix. Afterwards, the localization algorithms can be applied to the “cleaned” matrix.

$$s(f)=argmin\left\|R(f)-R_S(f)\right\|=argmin\left\|R(f)-s(f)(L(f,G)\,L(f,G)^H)\right\| \quad (11)$$

Conclusion

The results of the numerical simulations and the outdoor measurements lead to two major conclusions. One the one hand, they show that the free field assumption in DOA estimation with horizontal arrays and consequently the source range estimation with multiple arrays (by triangulation) is fully justified. Horizontal arrays are hardly influenced by the ground reflection and, as a result, do not suffer from the associated indirect effect of turbulence. They will still be prone to the direct effect of turbulence though, for low to medium turbulence, this will only be relevant for large propagation distances and large arrays not included in this study.

Source elevation, on the other hand, can't be reliably determined with a vertical array and free field DOA estimation because of the substantial effect of the reflection on the ground.
This effect can be exploited by combining classical source localization techniques like SRP and MUSIC with a simple, analytical propagation model. The combined approach (“ground effect inversion”) enables the user to fix the source range and elevation with a single array, even if the source is already in the far field, offering a very precise elevation estimation and a still moderate accuracy for the source distance. Spatial resolution depends mainly on the frequency relative to the array size, an eight element array with 20 cm spacing is usable for frequencies of above approx. 500 Hz. Resolution can be severely increased by use of superresolution techniques such as MUSIC.
Broadband processing proved to be favourable compared to narrowband processing, even though it may not offer higher spatial resolution is leads to a better defined maxima of the beamform power at the source position hence avoiding the search for its global maximum to be trapped in an unwanted local one.
Another benefit of ground effect inversion is that it allows to separate source which standard far field localization can't separate because of a too small difference in elevation. Nevertheless, one has to keep in mind that sources at a similar height are still difficult to be separated, especially if one source is substantially weaker than the other.
Sensitivity of the method with respect to noise and errors in the chosen ground impedance depends strongly – for a given array size – on the frequency range. One can expect acceptable repeatability for an SNR of more than 5 dB for the lowest frequency range considered (50 – 250 Hz), while – 5 dB or even -10 dB are sufficient for frequencies above 1 kHz. Higher frequencies also reduce the sensitivity towards an inaccurately chosen ground impedance. It is still recommended to refer to tables of ground parameters and make a careful choice in order to not make an error in the flow resistivity of a factors of two ore more.
If the method is to be used in the low frequency range and/or for low SNRs, there's always the option to increase the microphone spacing and/or the number of microphones, though this has obvious disadvantages from a practical point of view. Likewise, the simulations indicate that it's better to place the array more than 1 meter above the ground, with a height of 2 meters being a good compromise between increase in general performance and practicability.
The new procedure has not only advantages. Depending on the intended use, a major concern can be the much lower computational efficiency (2D search, calculation of sound field) compared to standard DOA estimation and the very efficient TDOA based position determination, particularly in case of broadband processing. In fact, TDOA based localization demonstrated a rather good performance, esp. with the large array. However, as the poor performance with the small array and larger source distances shows this is a nearfield method hence is not suited for larger source ranges. In addition, there's still the problem with multiple sources of similar level and nonuniqueness
of delay estimation in case of periodic signals. Furthermore, over highly reflecting
ground, one can no longer be sure that the estimated delays are actually the delays between the direct signals and not between any combination of direct signal and reflection. In this sense, ground effect inversion is more robust.
There remain a number of unanswered questions. One factor not considered is vertical sound speed gradients which, as shown, have a non negligible effect on DOA estimation. With a sufficiently high number of microphones it is, in theory, possible to simultaneously estimate not only the source position but also parameter(s) describing the sound speed profile (and the ground impedance), but one may well question the feasibility of such an approach involving a search over more than two dimensions and a more complicated sound field model. As long as one concentrates on higher frequencies such a strategy may still be viable if one uses raytracing.
Finally, a problem completely unaddressed is turbulence causing a remarkable variability in the (vertical) array's sound field and consequently position estimates with time. This may well limit the usefulness of ground effect inversion over hard ground and for larger source- array distances.

Acknowledgement

The authors would like to thank the German Research Foundation (DFG) for their support of this study.

References

[1] Fergusson, BG. (2002). “Locating far field impulsive sound sources in air by triangulation.” J. Acoust. Soc. Am. 111(1): 104-116

[2]Amar, A., Weiss, AJ. (2009). “Direct Position Determination: A Single-Step Emitter Localization Approach.” in: Tuncer, Friedlander (eds.). “Classical and Modern Direction-of-Arrival Estimation.” Academic Press.

[3] Bédard, J., Paré, S. (2003). “Ferret, A small arms' fire detection system: Localization concepts.” Sensors, and Command, Control, Communications, and Intelligence (C3I) Technologies for Homeland Defense and Law Enforcement II. Proceedings of SPIE 5071: 497-509

[4] Collier, S L., Wilson, DK. (2004). “Performance bounds for passive sensor arrays operating in a turbulent medium: Spherical-wave analysis.” J. Acoust. Soc. Am. 116(2): 987-1001

[5] Havelock, D I. et al. (1995). “Spatial coherence of a sound field in a refractive shadow: Comparison of simulation and experiment.” J. Acoust. Soc. Am. 98(4): 2289-2302

[6] Moran, ML. et al. (2007). “Acoustic array tracking performance under moderately complex environmental conditions.” Appl. Acoustics 68: 1241-1262

[7] Li, KM., Attenborough, K., Heap, NW. (1991). “Source height determination by ground effect inversion in the presence of a sound velocity gradient.” J. Sound Vib. 145: 111.128

[8] Nobile MA, Hayek SI. (1985). “Acoustic propagation over an impedance plane.” J. Acoust. Soc. Am. 78(4): 1325-1336

[9] Attenborough, K. (1992). "Ground parameter information for propagation modeling." J. Acoust. Soc. Am. 92(1): 418-427.

[10] ANSI S1.18-1999 (R2004). “Template Method for Ground Impedance.” American National Standards Institute.

[11] Kruse, R., Mellert, V. (2008). “Effect and minimization of errors in in situ ground impedance measurements.” Appl. Acoustics 69: 884–890.

[12] Salomons, EM. (2001). „Computational atmospheric acoustics.“ Kluwer Academic Publishers.

[13] Attenborough, K. et al. (1995). „Benchmark cases for outdoor sound propagation models.“ J. Acoust. Soc. Am. 97(1): 173-191

[14] Johnson, MA., Raspet, R. et al. (1987). "A turbulence model for sound propagation from an elevated source above level ground." J. Acoust. Soc. Am. 81(3): 638-646.

[15] Krim, H., Viberg, M. (1996). “Two decades of array signal processing research.” IEEE Signal Processing Magazine 13(4): 67-94

[16] Tuncer, TE., Yasar, TK., Friedlander, B. (2009). “Narrowband and Wideband DOA Estimation for Uniform and Nonuniform Linear Arrays.” in: Tuncer, Friedlander (eds.). “Classical and Modern Direction-of-Arrival Estimation.” Academic Press.

[17] Friedlander, B. (2009). “Wireless Direction-Finding Fundamentals.” in: Tuncer, Friedlander (eds.). “Classical and Modern Direction-of-Arrival Estimation.” Academic Press.

[18] DiBiase, JH. et al. (2001). “Robust localization in reverberant rooms.“ in: Brandstein, Ward (eds.). “Microphone arrays”, Springer

[19] ANSI S1.18-1999 (R2004). “Template Method for Ground Impedance.” American National Standards Institute

[20] Clifford, SF., Lataitis, RJ. (1983). "Turbulence effects on acoustic wave propagation over a smooth surface." J. Acoust. Soc. Am. 73(5): 1545-1550.

[21] Stoica, P., Moses, R. (2005). “Spectral analysis of signals.” Prentice- Hall: 326-331

Tables

f [Hz]	100	250	500	1000	2000
R [m]	15	25	50	100	
α [deg]	0	15	30	45	
Δd [cm]	5	10	20	50	
σ_e [krayl/m]	7.5	200	4000		
α_e [m^{-1}]	16	40	-115		

Table 1: Simulation of the influence of environmental conditions on DOA estimation with microphone arrays. Overview of parameter combinations. σ_e and α_e are paired.

SNR [dB]	**-20**		**-10**		**-5**		**0**		**5**		**10**		**20**	
	R	**α**	**R**	**α**	**R**	**α**	**R**	**α**	**R**	**α**	**R**	**α**	**R**	**α**
50 – 250 Hz	41	17	46	28	62	58	62	63	81	89	74	93	89	91
250 – 1000 Hz	41	25	54	69	66	92	75	95	80	95	85	97	95	99
1 – 2 kHz	45	35	64	86	73	95	81	97	88	96	91	97	97	98
2 – 4 kHz	50	50	76	95	83	99	92	99	95	99	99	99	99	100

Table 2: Influence of the SNR on the variability of the source position estimates for all combinations of geometries, microphone spacings and ground impedance in tab.1. Only arrays with a microphone spacing of at least λ/10 included. Values denote the percentage of combinations with an error in the source distance R of less than 10% or an error in elevation α of less than 0.5 deg. Lowest array microphone at a height of 1 meter.

σ_{error} [%]	**-50**		**-25**		**50**		**100**		**All**	
	R	**α**	**R**	**α**	**R**	**α**	**R**	**α**	**R**	**α**
50 – 250 Hz	59	65	81	91	74	88	62	72	75	83
250 – 1000 Hz	68	85	83	98	75	94	63	91	78	94
1 – 2 kHz	88	95	89	98	82	96	73	95	84	97
2 – 4 kHz	86	99	92	100	87	98	86	97	90	99

Table 3: Influence of the error in the ground's flow resistivity σ used for the position estimation on the estimation error. Only arrays with a microphone spacing of at least λ/10 included. Values denote the percentage of combinations with an error in the source distance R of less than 10% or an error in elevation α of less than 0.5 deg. Lowest array microphone at a height of 1 meter.

R [m]	α [deg]	100 Hz	250 Hz	500 Hz	1 kHz	Pink noise
15	10.1	0.0	7.0	9.8	7.0	7.3
15	10.1	0.0	7.8	9.3	7.0	7.0
15	1.8	0.0	0.0	0.0	0.0	0.0
15	1.8	0.0	0.0	0.0	0.0	0.0
24	6.4	0.0	20.3	0.0	4.8	4.5
24	6.4	0.0	20.0	0.0	4.8	4.5
24	1.1	0.0	0.0	0.8	0.0	0.0
24	1.1	0.0	0.0	1.0	0.0	0.0
40	3.8	0.0	5.3	0.3	2.8	2.8
40	3.8	0.0	7.0	0.5	3.0	3.5
40	0.7	0.0	1.0	1.8	0.0	0.0
40	0.7	0.8	1.0	2.3	0.0	0.0
Mean error		3.9	3.7	2.3	1.5	1.5

Table 4: DOA estimation with a vertical array for six different source positions and five source signals. Comparison of actual and estimated DOA. Two measurements for each geometry, the second one with a reduced source level. Last row shows mean absolute error in estimated elevation.

Actual position		Estimated source position									
		500 Hz		1 kHz		2 kHz		Pink noise		From TDOA	
R [m]	α [deg]	R	α	R	α	R	α	R	α	R	α
15	10.1	15.5	11.0	12.7	10.3	31.3	8.5	12.3	10.3	17.4	9.8
15	10.1	14.3	10.5	12.7	10.5	35.2	8.5	12.3	10.3	14.3	7.0
15	1.8	14.9	3.3	12.8	1.5	18.9	0.0	13.8	1.5	18.9	0.0
15	1.8	14.9	3.3	14.0	1.5	14.0	1.5	14.0	1.5	18.9	0.8
24	6.4	21.2	7.5	23.8	6.8	18.1	6.5	19.6	6.5	22.9	6.3
24	6.4	22.0	8.0	22.9	7.0	18.9	6.5	20.8	6.5	22.9	6.3
24	1.1	24.8	5.0	18.9	0.8	24.8	1.5	21.2	1.0	36.6	0.0
24	1.1	29.0	6.0	23.8	0.8	25.8	1.5	23.8	1.3	38.1	0.5
40	3.8	26.8	7.5	50.0	4.3	33.8	3.8	35.2	3.8	48.1	3.3
40	3.8	29.0	7.3	50.0	4.3	50.0	4.5	42.8	4.5	46.3	4.5
40	0.7	46.3	7.0	33.8	1.0	32.6	0.8	33.8	0.8	50.0	0.5
40	0.7	48.1	6.0	30.1	0.0	25.8	0.3	27.8	0.0	29.0	0.0
Mean error		4.2	2.9	4.2	0.4	7.7	0.6	3.7	0.3	6.3	0.8

Table 5: Source position detection with single vertical array. Comparison of actual position with estimates for different source signals. Two measurements for each geometry, the second one with a reduced source level. Last row shows mean absolute error.

Actual		Estimated (inversion)		Estimated (TDOA)		Estimated (DOA)
R [m]	α [deg]	R	α	R	α	α
15	10.1	13.8	9.5	14.9	8.8	2.3
15	1.9	13.3	1.5	14.3	1.0	0.0
15	3.8	13.3	3.3	14.9	2.5	0.0
24	2.4	19.6	1.5	26.8	0.3	0.0
24	1.2	19.6	0.8	22.9	0.0	0.0
40	0.7	27.8	0.8	32.6	0.0	0.0
40	1.4	29.0	0.5	31.3	0.0	0.0
15	1.9	13.3	1.0	15.5	0.0	0.0
40	0.7	30.0	0.0	27.8	0.0	0.0
24	1.2	19.6	1.0	22.0	0.0	0.0
Mean error		5.3	0.6	3.6	1.3	2.3

Table 6: Source position detection with single vertical array and three localization algorithms. Comparison of actual position with estimates for an eight element array with 50 cm spacing and a single source. Last row shows mean absolute error.

Figures

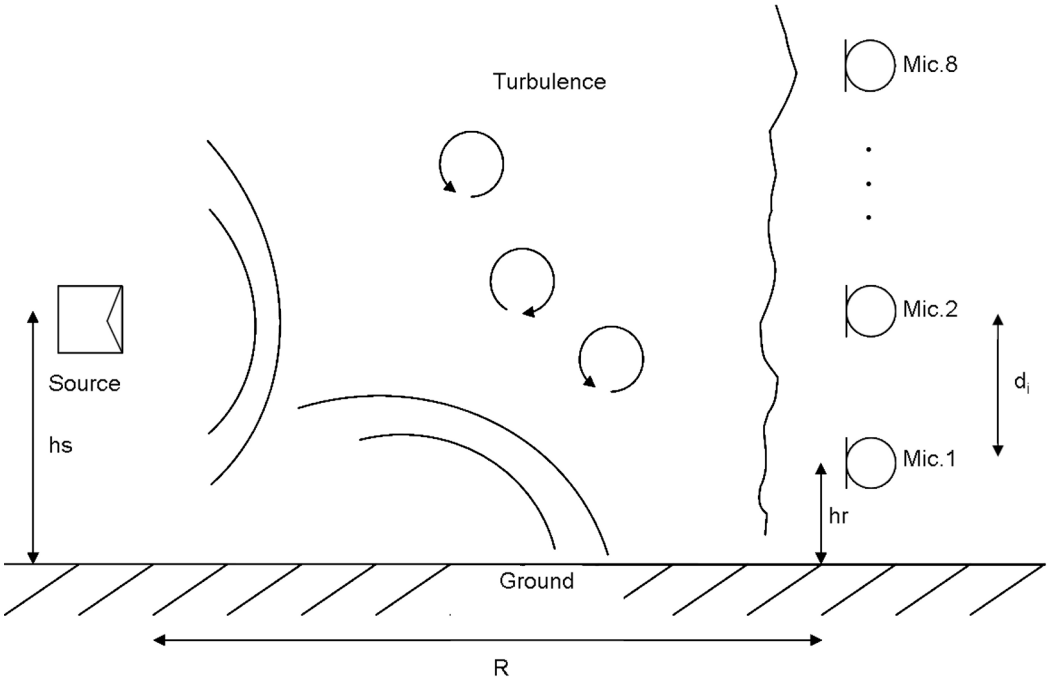

Figure 1: Sketch of the measurement set-up showing the influence of ground reflection, vertical sound speed gradient and turbulence on the wavefront arriving at the (vertical) array.

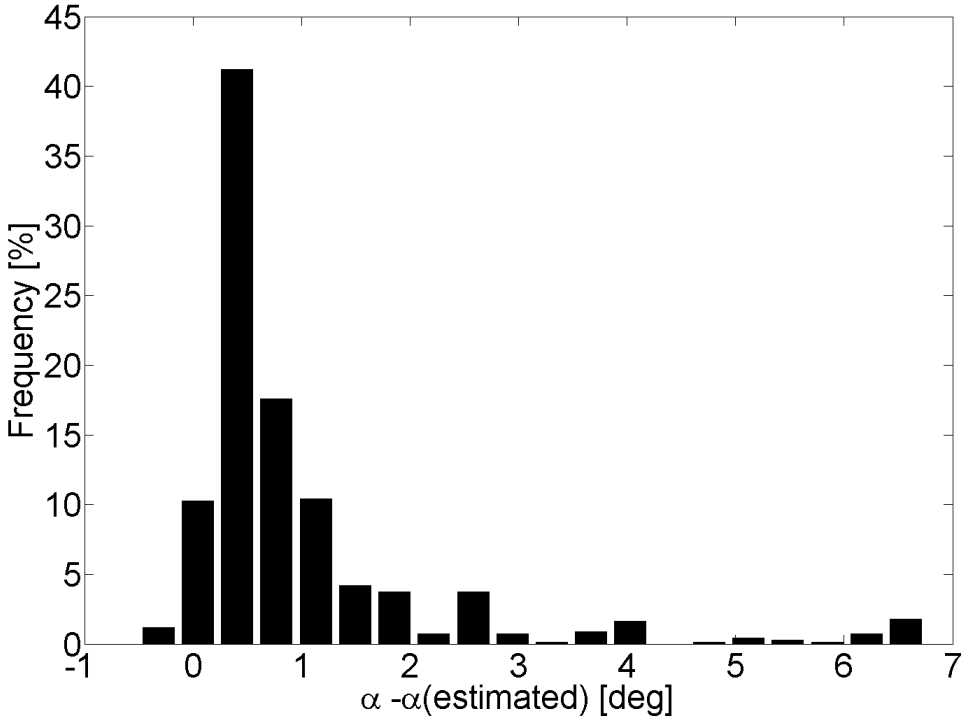

Figure 2: Distribution of DOA estimation errors for horizontal arrays due to ground reflections and near-field effect.

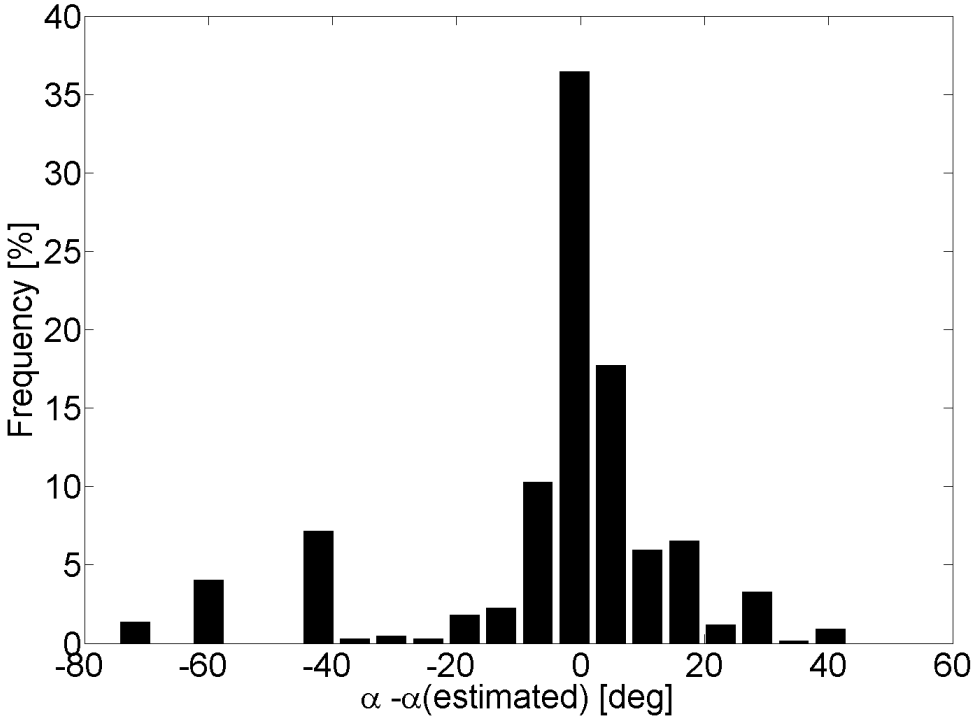

Figure 3: Distribution of DOA estimation errors for vertical arrays due to ground reflections and near-field effect. Notice the much larger range compared to horizontal arrays.

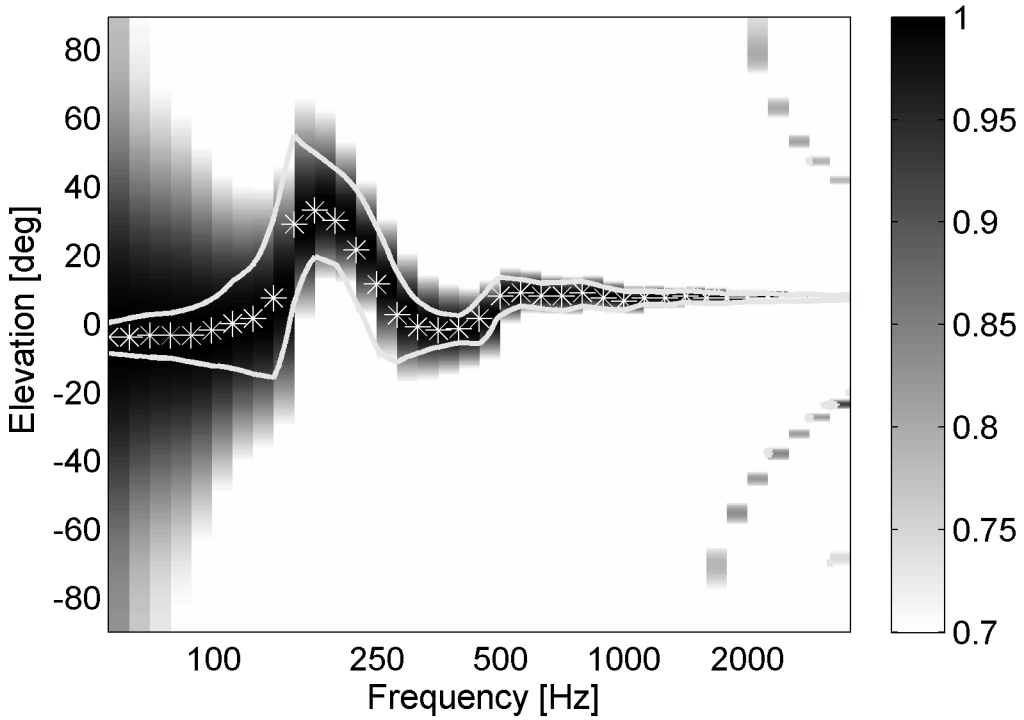

Figure 4: Normalized beamform power vs. frequency for a source-array distance of 15 m, an elevation of 10.1 deg and an array of 8 microphones with 20 cm spacing 1 meter above the ground. Pink noise mixed with spatially white noise at 10 dB SNR. DOA estimates for the frequency bands marked by (*). Line marks the corresponding area for φ_{MUSIC} = 0.7.

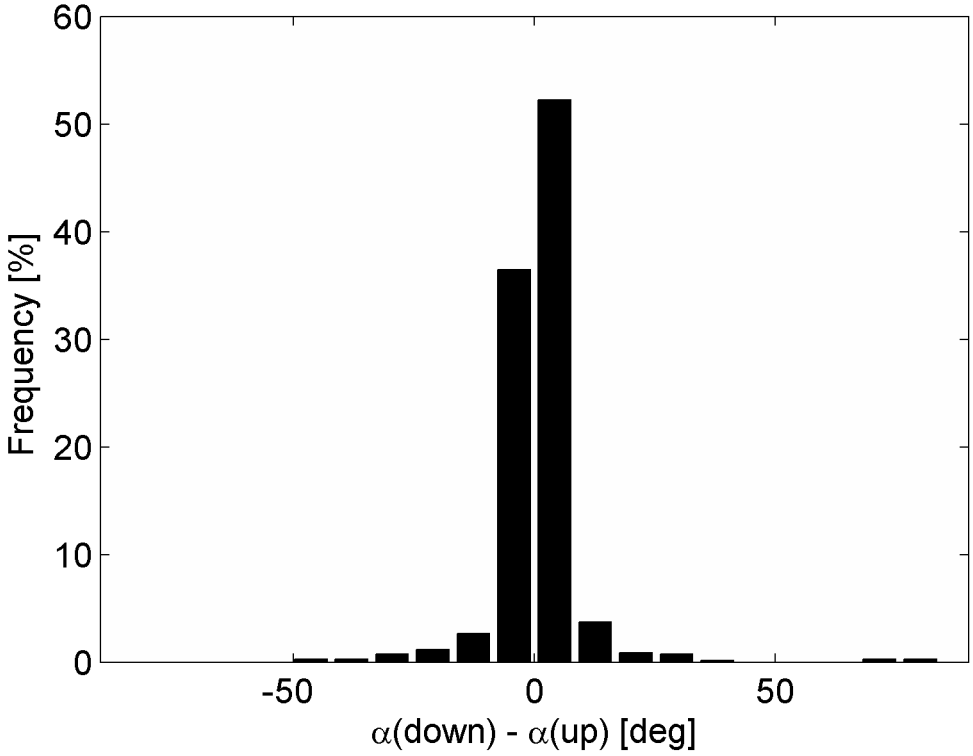

Figure 5: Distribution of differences in DOA estimates for a downward refracting (α_{down}) and an upward refracting (α_{up}) atmosphere.

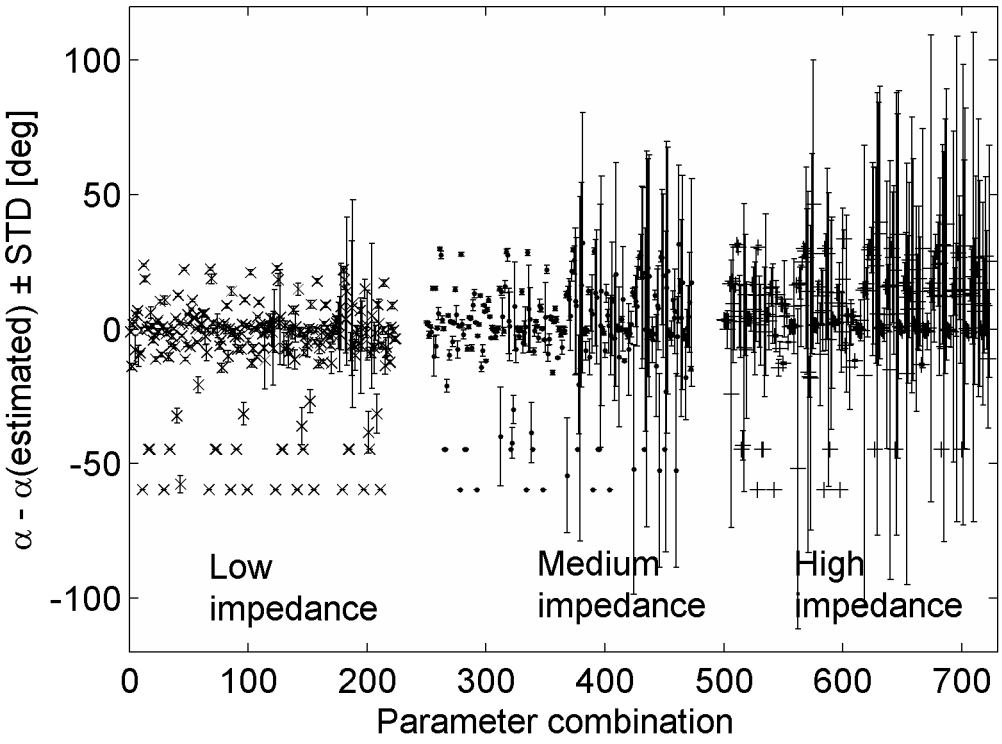

Figure 6: DOA estimation errors due to ground reflection, downward refracting atmosphere and turbulence for three different ground impedances. Average and standard deviation for 25 realizations of the turbulent field. Source- array distance increases stepwise from left to right. Variability increases considerably with increasing ground impedance and distance.

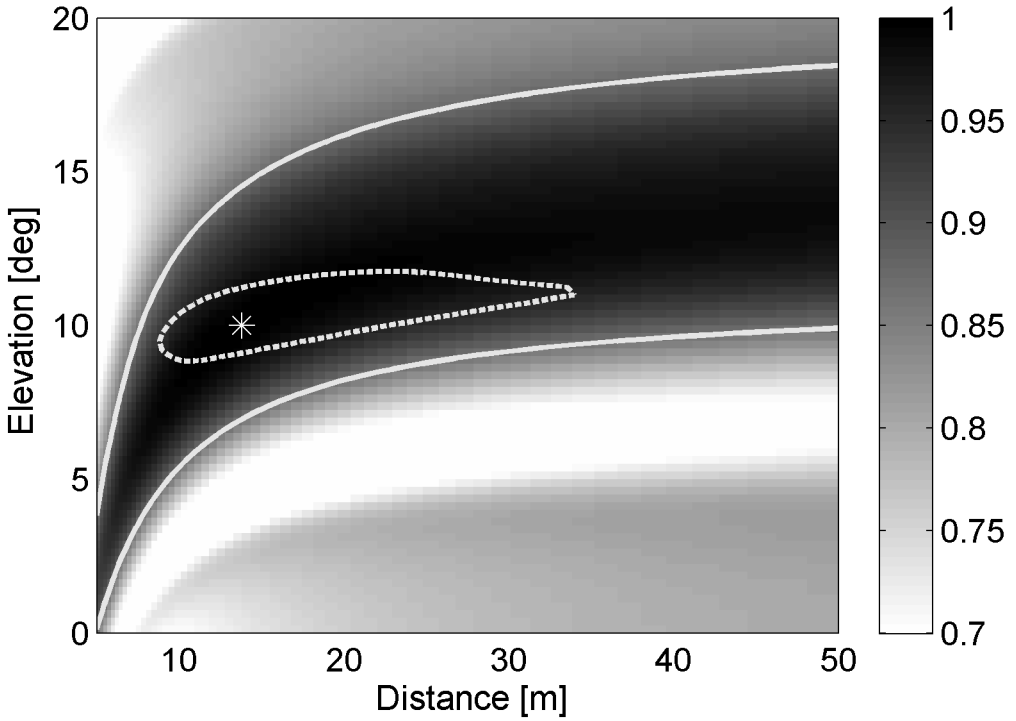

Figure 7: Beamform power vs. position for a source at a distance of 15 m and an elevation of 10.1 deg. Source emits a 250 Hz signal, SNR is 10 dB. Vertical array of 8 microphones with a 20 cm spacing. Estimated source position is marked by (*). Line marks corresponding area for φ_{MUSIC} = 0.7, dashed line area for φ_{MUSIC} = 0.7 and a 50 cm microphone spacing.

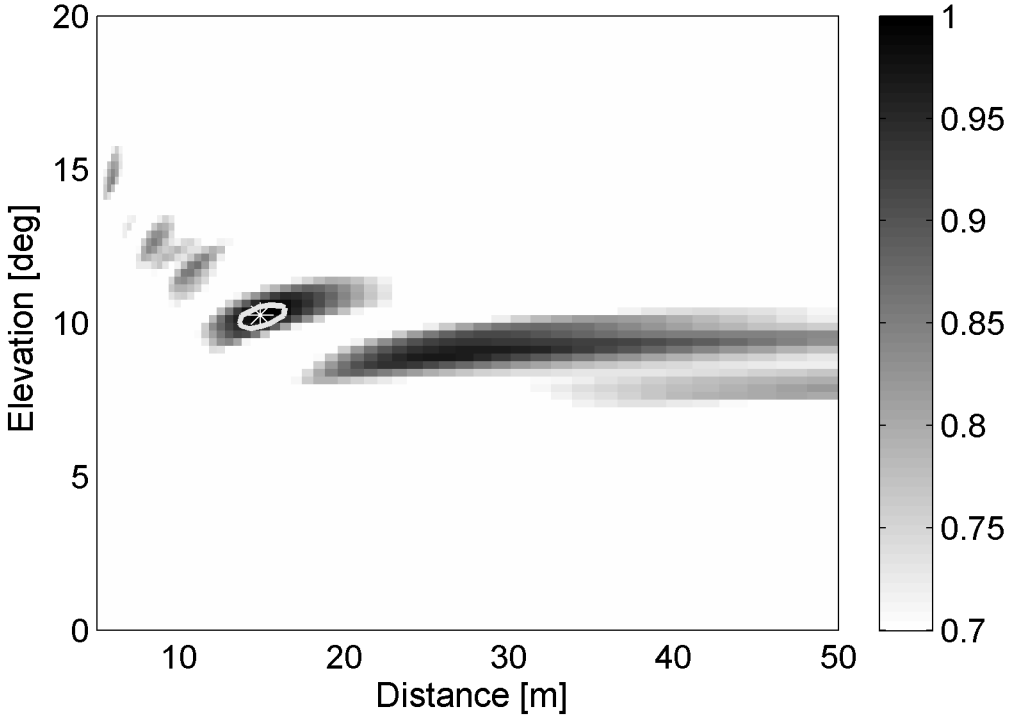

Figure 8: Beamform power versus position for a source at a distance of 15 m and an elevation of 10.1 deg. Source emits a 2 kHz signal, the SNR is 10 dB. Estimated source position is marked by (*). Ellipses mark corresponding area for φ_{MUSIC}. Notice the extended local maximum at 30 m distance.

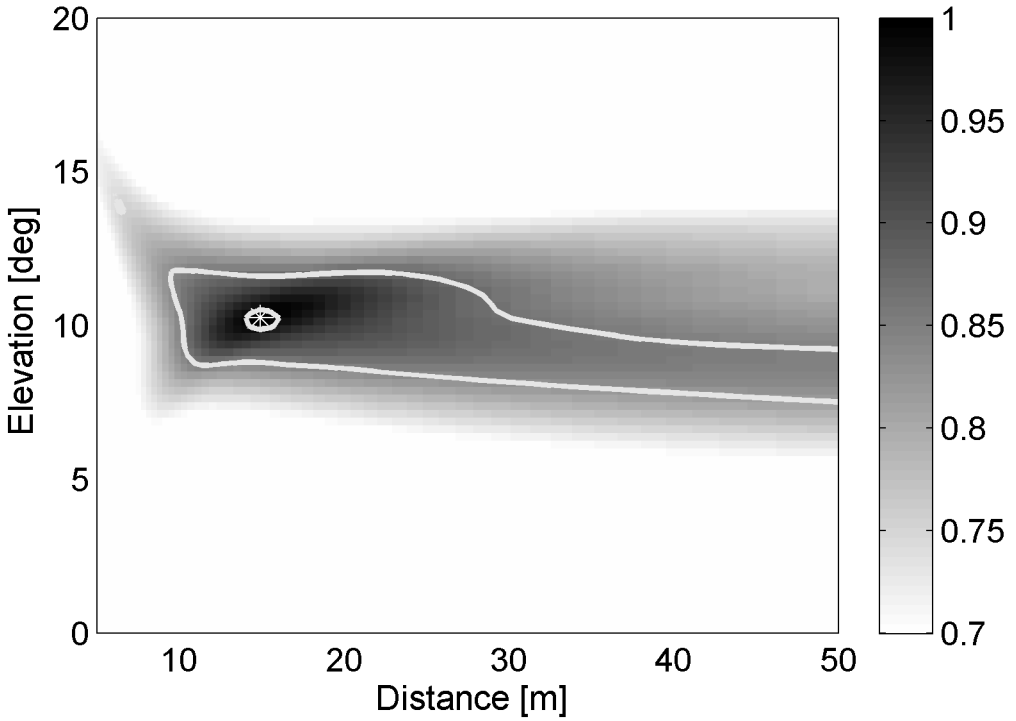

Figure 9: Beamform power versus position for a source at a distance of 15 m and an elevation of 10.1 deg. Source emits pink noise between 50 and 4000 Hz, the SNR is 10 dB. Estimated source position is marked by (*). Line marks the corresponding area for pink noise between 500 – 4000 Hz, ellipses the respective areas for $\varphi_{MUSIC} = 0.7$.

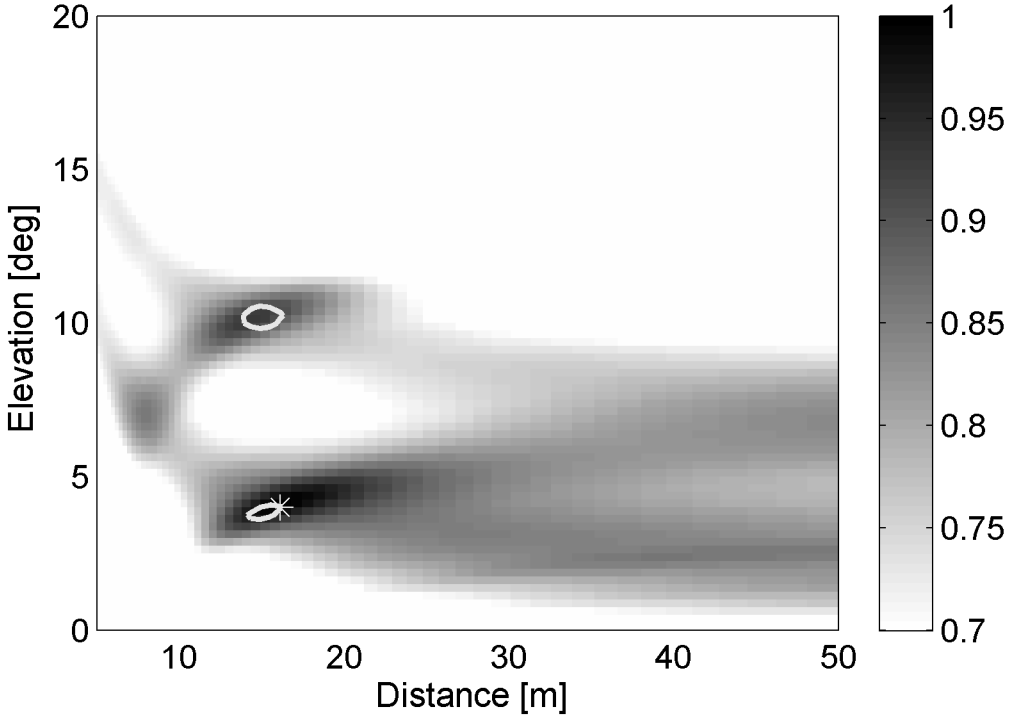

Figure 10: Beamform power versus position for two sources at a distance of 15 m and an elevation of 3.8 deg resp. 10.1° . Sources emit pink noise between 500 and 4000 Hz, the SNR is 10 dB. Estimated (strongest) source position is marked by (*). Ellipses mark the corresponding area for $\varphi_{MUSIC} = 0.7$.

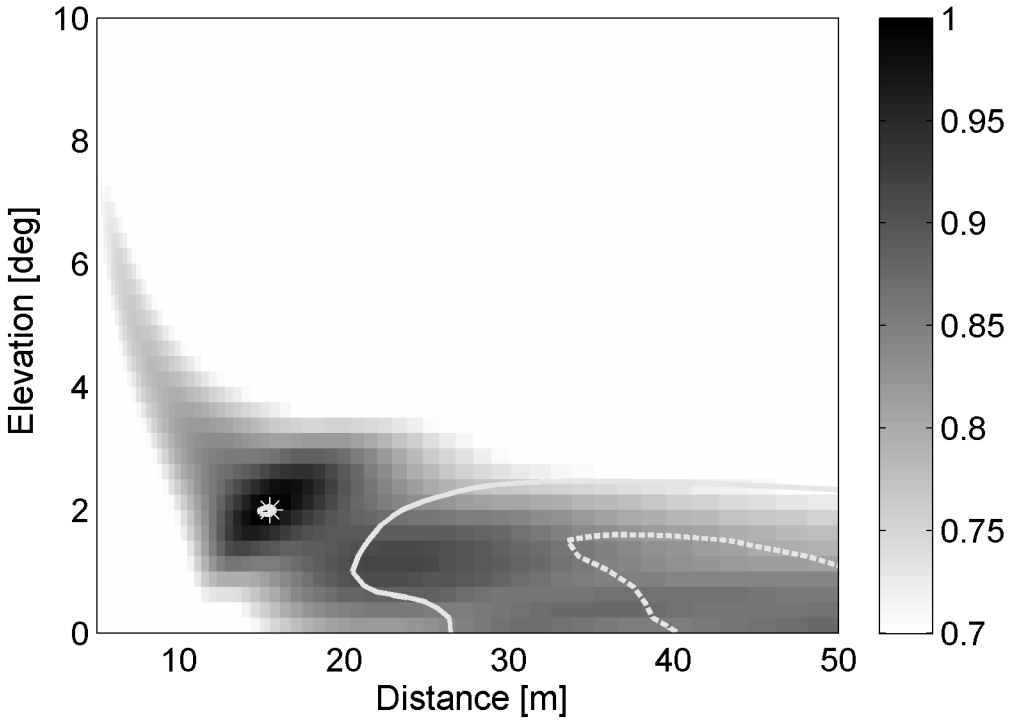

Figure 11: Beamform power versus position for two sources at a distance of 15 and 24 m and an elevation of 1.9 resp. 1.2 deg. Sources emit pink noise between 500 and 4000 Hz, the SNR is 10 dB. Estimated (strongest) source position is marked by (*). Line marks the corresponding areas for φ_{MUSIC} = 0.5, dashed line φ_{MUSIC} = 0.9.

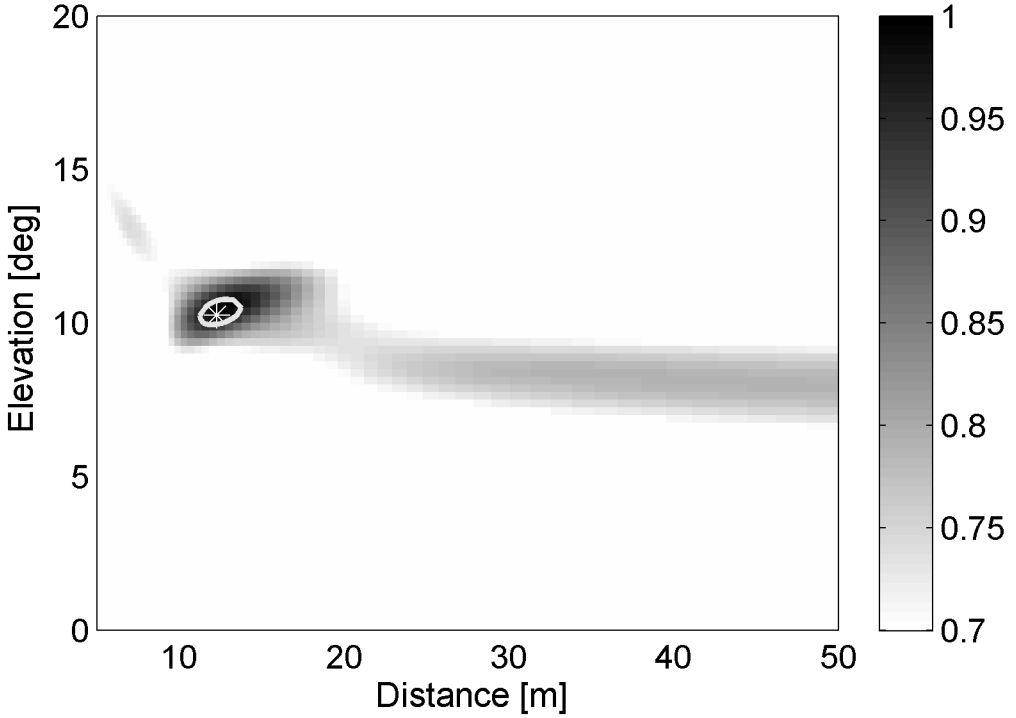

Figure 12: Measurement: beamform power versus position for a sources at a distance of 15 m and an elevation of 10.1 deg. Microphone spacing is 20 cm. Pink noise between 500 and 4000 Hz, the SNR is 18 dB. Estimated source position is marked by (*). Ellipse marks the corresponding area for φ_{MUSIC} = 0.7.

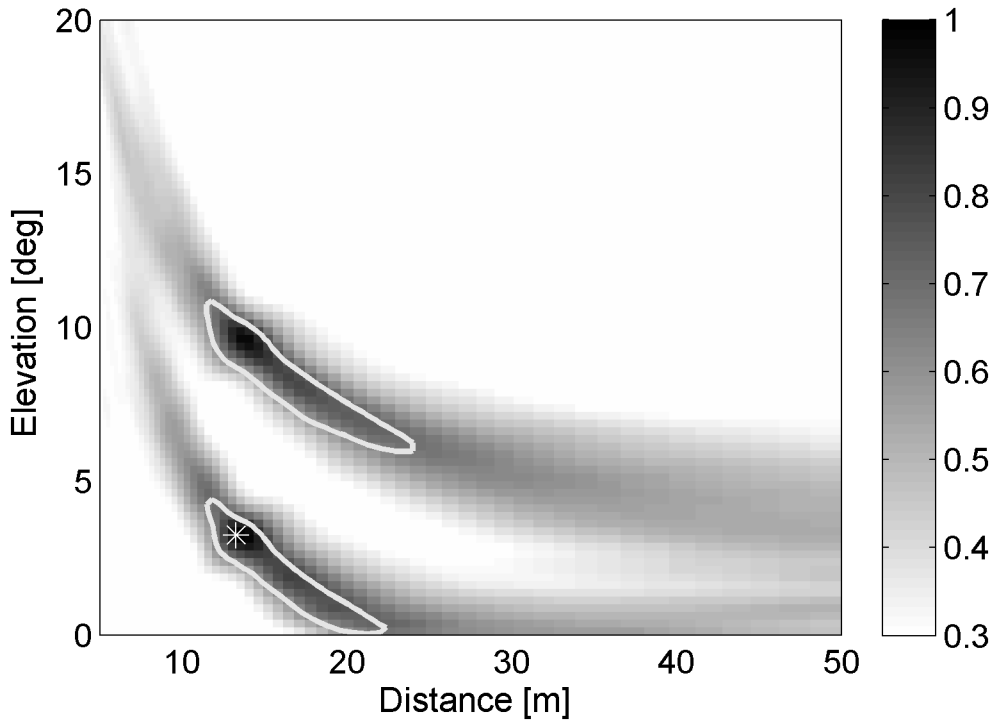

Figure 13: Measurement: normalized beamform power versus position for two sources of equal power emitting uncorrelated pink noise between 500 and 4000 Hz. First source at 15 m and 10.1 deg elevation, second source at 15 m and 3.8 deg. Total SNR is 18 dB. Ellipse marks the corresponding area for φ_{MUSIC} = 0.3.

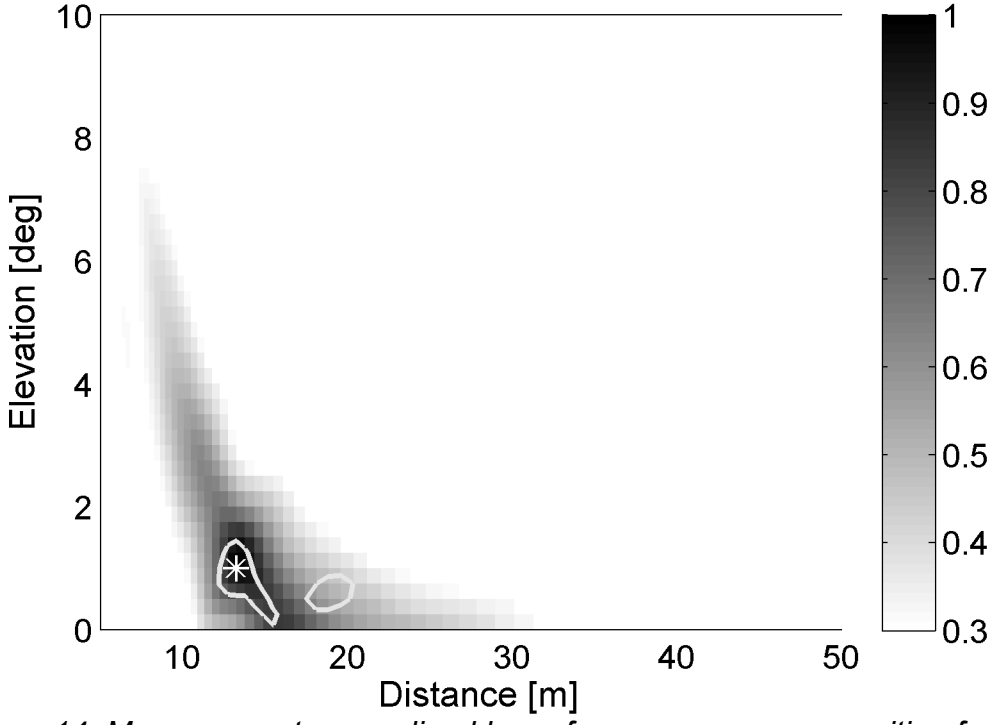

Figure 14: Measurement: normalized beamform power versus position for two sources of equal power emitting uncorrelated pink noise between 500 and 4000 Hz. First source at 15 m and 1.9 deg elevation, second source at 24 m and 1.2 deg (6 dB lower power). Total SNR is 18 dB. Ellipse marks the corresponding area for φ_{MUSIC} = 0.6.

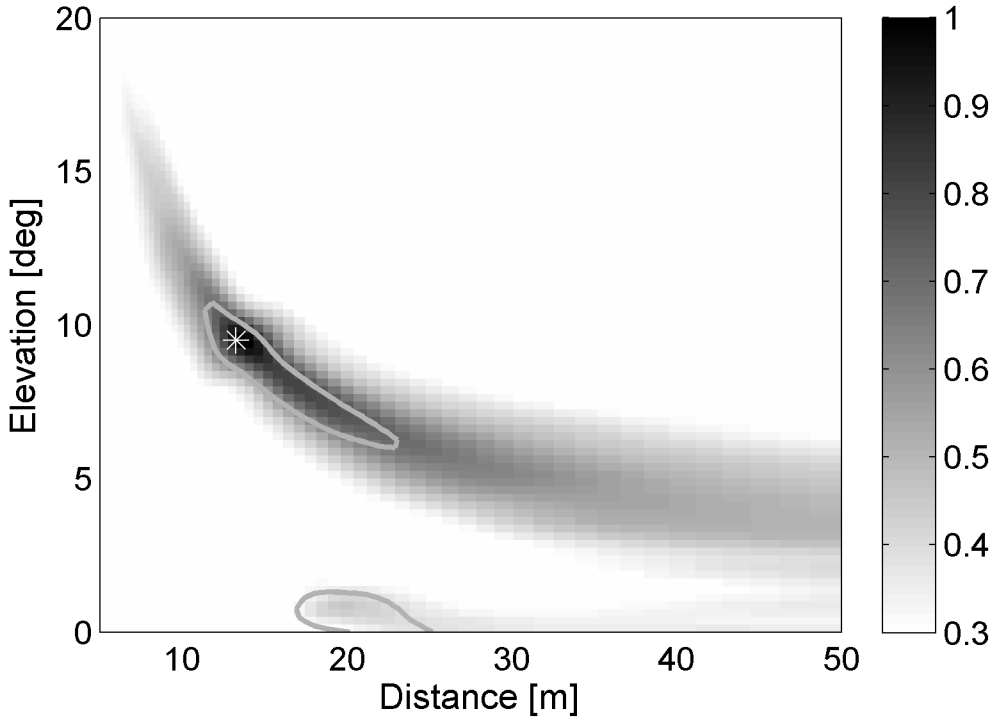

Figure 15: Measurement: normalized beamform power versus position for two sources of equal power emitting uncorrelated pink noise between 500 and 4000 Hz. First source at 15 m and 10.1 deg elevation, second source at 24 m and 1.2 deg (6 dB lower power). Total SNR is 14 dB. Ellipse marks the corresponding area for $\varphi_{MUSIC} = 0.3$.